Available online at www.sciencedirect.com
SCIENCE DIRECT®
International Journal of Heat and Mass Transfer 47 (2004) 1525–1533
International Journal of HEAT and MASS TRANSFER
www.elsevier.com/locate/ijhmt

Vapor absorption by immobile solution layer

V.E. Nakoryakov *, N.S. Bufetov, N.I. Grigorieva, R.A. Dekhtyar, I.V. Marchuk

Institute of Thermophysics, Russian Academy of Sciences, Novosibirsk, 630090, Russia

Abstract

Using simple models of nonisothermal absorption for small and long times, the effect of heat release and heat drain on intensity of vapor absorption by immobile solution layer was analyzed. The models consider the case of moving and steady interface. The experimental results of water vapor absorption by immovable water solution of LiBr are presented. The temperature evolution curves are given for different levels of solution, as well as temperature and concentration profiles. Calculation data was compared with experiment.

Keywords: Absorption; Heat pump; Heat and mass transfer; Analytic solutions; Heat release; Heat removal; Displacement of phase interface

1. Introduction

Vapor absorption by salt solutions with intensive heat release is used widely in design of heat pumps and absorption cooling machines. Usually the absorption process occurs on surfaces of the falling liquid films with heat removal through a solid wall. Therefore, most of papers deal with film absorption. For example, in [1–5] the authors use simple models of nonisothermal absorption for accurate analytical solutions, and self-similar as well [2,5]. Results of simulation were presented in [6–17]. Experimental study of film absorption and comparison of calculations with experimental data was presented in [18–24].

Modern requirements to development of high-performance apparatus initiate the search for new methods of transfer process intensification in absorbers. One of the methods for absorption enhancement is use of surfactant additives; these additives facilitate development of low-scale surface convection and, as the result, intensify heat and mass transfer. However, in experiments on the effect of surfactant species on intensity of film absorption it is rather difficult to distinguish the contribution of the main flow and the convection due to a surface tension gradient. In this case, the convenient object for research could be vapor absorption by immobile solution layer (there is no forced flow here) [25]. For this arrangement, all theoretical and experimental data on characteristics of heat and mass transfer during absorption without surfactants could be a comparison standard for the results on absorption in a solution with surfactant. In [25] this comparison was conducted only for one integral characteristics (for time evolution of the mass of absorbed substance). The process of vapor absorption by a steady layer of solution is a convenient object for theoretical study because one can estimate the contribution of every factor of mass and heat transfer: heat release, movement of the interface, heat loss through the wall, and effect from surfactant in solution. Besides, after several additional assumptions one can obtain simple analytical solutions [26,27] for most of these factors (except the presence of surfactant in solution); these data are convenient for analysis and comparison with experimental data. Moreover, in absorption of vapor by immobile layer of liquid creates experimental conditions very close to theoretical models.

2. Model of nonisothermal absorption

The heat and mass transfer problem for a binary solution were considered under the following list of

* Corresponding author. Tel.: +7-383-234-4276; fax: +7-383-234-3480.
E-mail address: nakve@itp.nsc.ru (V.E. Nakoryakov).

0017-9310/$ - see front matter © 2003 Elsevier Ltd. All rights reserved.
doi:10.1016/j.ijheatmasstransfer.2003.10.017

Nomenclature

a	thermal diffusivity
C	absorbate concentration (mass fraction) in solution
D	diffusivity
K	phase transition criterion
Le	Lewis' number
m_a	mass flux density
P	pressure
r_a	latent heat
T	temperature
t	time
V	interface displacement velocity
x	transverse coordinate

Greek symbols

δ	layer thickness
γ	dimensionless concentration
η	dimensionless coordinate
λ	thermal conductivity coefficient
θ	dimensionless temperature
ρ	density of solution
τ	dimensionless time
ξ	self-similar variable

Subscripts

w	wall
0	value at $t = 0$
i	vapor–liquid interface
a	first component of solution (absorbate)
b	second component of solution (absorbent)
e	equilibrium values

assumptions which are valid, in particularly, for systems used in absorption heat pumps and cooling machines:

- for the entire range of temperature and concentrations during absorption process the solution density remains constant, as well as all the parameters characterizing the thermophysical properties and transfer coefficients;
- vapor pressure is steady during absorption process;
- the heat of absorption is released at the interface and spent only for heating of liquid phase (solution);
- the temperature of the bottom surface T_w is kept constant and (in general case) can be different from the initial temperature of solution T_0;
- the solution consists of two components: one component is absorbed from the gas medium contacting with solution, and the second component is not consumed and not added into solution. Therefore, the interface is impermeable for the second component of solution and it moves with the velocity $V(t)$;
- the system vapor–solution is in equilibrium at the interface; for a constant pressure and binary solution this equilibrium is described by the dependency of concentration of absorbed substance on temperature $C = f(T)$. For small intervals of temperature and concentrations this relationship can be approximated by a linear function $C_i = k_1 - k_2 T_i$, with pressure-dependent coefficients k_1 and k_2;
- the absorption-caused heat with time causes changes in the equilibrium temperature at the interface, so changing the equilibrium concentration according to the relationship. Thus, the point with coordinates (C_i, T_i) shift along the equilibrium curve. But at every time moment, including the primary one, the position of this point is unknown a priory.

According to the listed assumptions, the joint heat and mass transfer in the solution layer can be described by conservation equations for mass and energy; they can be written down in the coordinate system originated from the moving boundary

$$\frac{\partial T}{\partial t} + V \cdot \frac{\partial T}{\partial x} = a \cdot \frac{\partial^2 T}{\partial x^2}, \quad \frac{\partial C}{\partial t} + V \cdot \frac{\partial C}{\partial x} = D \cdot \frac{\partial^2 C}{\partial x^2}$$

with initial conditions at $t = 0$, $T = T_0$,

$$C = C_0,$$

and conditions on the interface for $x = 0$, $C_i = f(T_i)$,

$$-\lambda \frac{\partial T}{\partial x} = r_a \cdot m_a, \tag{1}$$

and the boundary conditions on the bottom surface for $x = \delta(t)$, $T = T_w$,

$$\frac{\partial C}{\partial x} = 0.$$

Here $V(t) = -\frac{D}{1-C_i}\frac{\partial C}{\partial x}$ (at $x = 0$) is the velocity of boundary motion, determined by impermeability condition for the second component of the solution

$$m_b = (1 - C_i) \cdot \rho \cdot V - \rho \cdot D \frac{\partial (1 - C)}{\partial x} = 0,$$

and m_a is the mass flux density for the absorbed component

$$m_a = C_i \cdot \rho \cdot V - \rho \cdot D \frac{\partial C}{\partial x} = -\frac{\rho D}{1 - C_i} \frac{\partial C}{\partial x}.$$

3. Solution for small times

In papers [26,27] the authors considered the absorption process for times when heat transfer through the bottom does not influence the temperature evolution near the interface; i.e., the thermal boundary layer formed from the interface had not met yet the boundary layer developed from the solid wall (bottom). Moreover, the systems were considered with Lewis number $Le = D/a$ much smaller than one, so the thickness of the diffusion boundary layer is small (much less than the thermal layer thickness). In this way, this approach is applied to systems at small times or with a thick layer of solution.

For this case, the equation system and boundary conditions can be written in dimensionless form with using of the self-similar variable $\xi = \frac{x}{2\sqrt{at}}$:

$$\begin{aligned}
&\frac{d^2\theta}{d\xi^2} + 2\left(\xi + \frac{\sqrt{Le\cdot D\cdot t}}{1-C_i}\cdot\left.\frac{\partial C}{\partial x}\right|_{x=0}\right)\frac{d\theta}{d\xi} = 0,\\
&Le\frac{d^2\gamma}{d\xi^2} + 2\left(\xi + \frac{\sqrt{Le\cdot D\cdot t}}{1-C_i}\cdot\left.\frac{\partial C}{\partial x}\right|_{x=0}\right)\frac{d\gamma}{d\xi} = 0,\\
&\xi\to\infty,\quad \theta = 0,\ \gamma = 0,\\
&\xi = 0,\quad \gamma_i = F(\theta_i),
\end{aligned} \tag{2}$$

$$\frac{d\theta}{d\xi} = K\cdot Le\cdot\frac{(C_e - C_0)}{1-\gamma_i\cdot(C_e-C_0)-C_0}\cdot\frac{d\gamma}{d\xi}. \tag{3}$$

Here

$$\theta = \frac{T-T_0}{T_e-T_0};\quad K = \frac{r_a}{C_p\cdot(T_e-T_0)};\quad Le = \frac{D}{a};$$
$$\gamma = \frac{C-C_0}{C_e-C_0};\ C_e = f(T_0),\ C_0 = f(T_e).$$

The distributions for temperature and concentration are determined by solutions:

$$\theta = \frac{\theta_i\cdot[1-\operatorname{erf}(\xi+B)]}{1-\operatorname{erf}B},\quad \gamma = \frac{\gamma_i\cdot\left[1-\operatorname{erf}\left(\frac{\xi\backslash B}{\sqrt{Le}}\right)\right]}{1-\operatorname{erf}\left(\frac{B}{\sqrt{Le}}\right)}, \tag{4}$$

where

$$B = \frac{\sqrt{Le\cdot D\cdot t}}{1-C_i}\cdot\left.\frac{\partial C}{\partial x}\right|_{x=0},$$

and constants γ_i, θ_i, and B are independent on t and can be determined by the system of Eqs. (2)–(4).

If the equilibrium condition is approximated by linear function $C_i = k_1 - k_2 T_i$ with the angular coefficient $k_2 = \frac{C_e-C_0}{T_e-T_0}$, then (2) takes the form: $\theta_i + \gamma_i = 1$, and constant B can be found from the equation

$$B = -\frac{\sqrt{Le}(C_e-C_0)\cdot\gamma_i\cdot\exp\left(-\frac{B^2}{Le}\right)}{\sqrt{\pi}\cdot[1-\gamma_i\cdot(C_e-C_0)-C_0]\cdot\left[1-\operatorname{erf}\left(\frac{B}{\sqrt{Le}}\right)\right]},$$

where the dimensionless concentration on the interface is also expressed through the constant B,

$$\gamma_i = 1 + K\cdot B\cdot(1-\operatorname{erf}B)\cdot\sqrt{\pi}\cdot\exp(B^2).$$

Thus, we have equation for B in the form of $B = f(B)$; that kind of equation can be solved by iterations.

The mass flux density on the layer surface is found from the formula

$$m_a = \frac{\rho\sqrt{D}\cdot(C_e-C_0)}{\sqrt{\pi\cdot t}}\cdot\frac{\gamma_i}{1-\gamma_i\cdot(C_e-C_0)-C_0}\cdot\frac{\exp\left(-\frac{B^2}{Le}\right)}{1-\operatorname{erf}\left(\frac{B}{\sqrt{Le}}\right)}, \tag{5}$$

Comparison of (5) with similar formula for isothermal absorption [27] demonstrates that heat release and movement of the interface is taken into account by the two last multipliers.

4. Absorption with heat transfer (long times)

If the temperature of the bottom boundary of the layer T_w is kept constant, lower or equal to the initial temperature of solution T_0, then, in due course, the influence of the cold wall spreads up to the interface and the temperature profile becomes close to linear. This problem (without movement of the interface) was considered in [27]. The problem can be modified: we do not take into account motion of the interface in the diffusion equation and hold the convective component of mass flux in the boundary condition (1). This results in

$$\begin{aligned}
&\theta = \theta_i - (\theta_0+\theta_i)\cdot\eta,\quad \eta = \frac{x}{\delta},\ \theta_0 = \frac{T_0-T_w}{T_e-T_0},\\
&\frac{\partial\gamma}{\partial\tau} = Le\frac{\partial^2\gamma}{\partial\eta^2},\quad \tau = \frac{at}{\delta^2}.
\end{aligned} \tag{6}$$

Here the time is counted from the moment τ_0 when the temperature profile is almost linear.

The unknown values of temperature and concentration on the interface are related by the condition of equilibrium and heat balance:

$$\begin{aligned}
&\eta = 0,\quad \gamma = \gamma_i(\tau),\quad \theta = \theta_i(\tau),\quad \theta_i + \gamma_i = 1,\\
&\frac{\partial\theta}{\partial\eta} = \frac{K\cdot Le\cdot(C_e-C_0)}{1-\gamma_i(C_e-C_0)-C_0}\cdot\frac{\partial\gamma}{\partial\eta}.
\end{aligned}$$

Assuming that γ_i decays slowly with time, and that at the initial time moment it was equal to γ_{i0} (the dimensionless concentration on the interface at small time), then the estimates can be obtained from the solution presented in [27] for the case of steady interface.

Then

$$\gamma_i = 1 + \theta_0 - (1 - \gamma_{i0} + \theta_0) \cdot \exp(p\tau)(1 - \operatorname{erf}\sqrt{p\tau}),$$
$$\theta_i = 1 - \gamma_i; \tag{7}$$

where

$$p = \frac{[1 - \gamma_{i0}(C_e - C_0) - C_0]^2}{K^2 \cdot Le \cdot (C_e - C_0)^2}$$

and for every next time step we can use as γ_{i0} the value of γ_i calculated at the previous step.

There is a simple formula for mass flux density through the layer surface:

$$m_a = -\frac{\rho \cdot D}{1 - C_i} \cdot \left.\frac{\partial C}{\partial x}\right|_{x=0} = -\frac{\lambda}{r_a}\frac{\partial T}{\partial x} = \frac{\rho \cdot a}{\delta \cdot K}(\theta_0 + \theta_i).$$

These analytical ratios for short and long time intervals can be used for estimation of the effect of heat release and heat drain on absorption intensity, and can be useful in analysis of experimental results and to be a reference point for comparison of experimental and simulation data obtained for more complex conditions (for example, with presence of surfactant in solution).

5. Experimental setup and methods

Experiments were carried out at the setup (Fig. 1) consisting of absorber *1* and vapor generator *2* connected by a pipeline with quick-acting valve *3*. Water solution of lithium bromide (LiBr) was used as the absorber and steam was used as the absorbent. This system is widely used in absorption heat pumps and refrigerating machines. Its thermal physical and other properties have been studied perfectly and they are presented in [28].

The absorber was a cylindrical vessel of the 165-mm diameter and 87-mm height made of stainless steel with a lateral inspection window for visual control and measurements of the layer level, which were performed by cathetometer *6* with the accuracy of less than 0.01 mm. Thickness of absorber lateral walls was 1.5 mm and bottom thickness was 6 mm. Absorber walls were lined from inside with sheet Teflon of the 5-mm thickness to reduce possibility for development of convective flows along the walls.

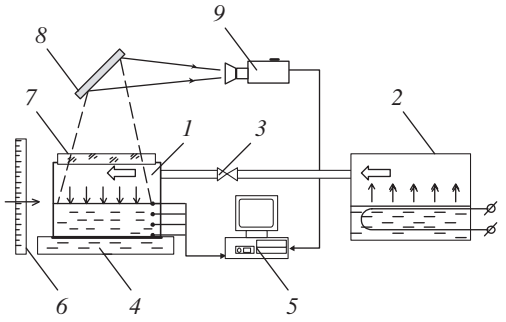

Fig. 1. General diagram of the experimental setup. 1—absorber, 2—vapor generator, 3—valve, 4—water thermostat, 5—computer, 6—cathetometer, 7—LiF glass, 8—sweeping mirror, 9—IR camera.

A vessel with a volume of about 20 l served as the vapor generator, there were heaters for water evaporation from LiBr solution on the bottom of this vessel. The computer control of the power source allowed the system pressure to be constant with the accuracy of ±5 Pa, i.e., it was possible to use the vapor generator as the barostat, and this was controlled by the difference membrane pressure probe with a low limit.

Five thermocouples in protection shells in the form of capillary tubes of 1-mm diameter were introduced along the radius through the lateral walls into the absorbent layer, where they were located with a horizontal shift relative to each other by 36° with a width step of 5 mm. The length of horizontal part of thermocouples inside the vessel was 65 mm. The lower capillary was near the bottom and touched it, and the upper one was located on the height of 20 mm. The absorber was filled with concentrated solution of LiBr in the amount (0.855 ± 0.025 kg) sufficient to cover the shell of upper thermocouple by the layer of 0.2–0.5 mm.

Thermocouples were made of copper and constantan wires with diameters of 0.16 and 0.1 mm. Individual calibration allowed temperature measurements with an error not higher than 0.1 °C. At step change of the temperature, the thermocouple readings reached constant values for the period not longer than 3 s.

Measurements of the surface temperature of lithium bromide were carried out using infrared (IR) camera *9*. A single-element cadmium–mercury–tellurium photodiode cooled by liquid nitrogen served as the radiation detector. The registered range of IR radiation was 3.5–5.5 μm, and this allowed receiving of main radiation from the depth of about 10 μm. Scanning was performed mechanically by two rotating germanium prisms. Radiation from the surface of lithium bromide solution passed through window *7* reflected from sweeping mirror *8* and came to the objective of IR camera. The window transparent for IR radiation was LiF glass with the diameter of 140 mm and thickness of 20 mm. The scanner might operate in two modes. Under an ordinary mode, frame-by-frame scanning was performed with a rate of 1 frame per 1.2 s. The time between frames was 1.91 s. The frame size was 192×192 of an element. Under the second mode, scanning was performed without frame sweeping, and the frame prism did not rotate. Actually, the temperature of solution surface was measured along a given line. The scanning time for one line was 0.0061 s. Therefore, frequency of temperature measurements under the second mode was 164 Hz. To

calibrate the device, two standard emitters with different temperature were put to the viewing field of the IR camera. The emitters were cylinders of the 10-mm diameter and 10-mm height made of copper. There was a microheater inside one of them. The emitting surfaces of these cylinders were blackened with lamp soot. Their temperatures were measured by thermocouples. The value of a signal measured by photodiode was recalculated to the value of temperature using Plank formula for radiation of a blackbody in accordance with the temperature of standard emitters. Radiation coefficients of standard emitters and surface of lithium bromide solution were assumed the same. Measurement error was estimated as ±0.25 °C.

To measure the heat flux, differential thermocouples were mounted into the absorber bottom at distances of 0.5 and 5 mm from the bottom surface.

To obtain data on distribution of solution concentration, samples were taken from different levels of the layer. Samplers were tubes of the 2-mm diameter with blocked ends and holes of the 0.8-mm diameter drilled in their lateral walls. Sampling tubes were located to take the solution from a given level, and their holes were directed upward. This position provided minimal mixing of solution at layer-by-layer drain.

Before the experiment, the absorber was covered by a special cap of polyethylene film, and all space under this cap was kept at a constant temperature. For this purpose, an electric heater with fan and temperature probe, controlled by PC, was located there. A fan provided constant air circulation under the cap, and the heater maintained the air temperature around absorber over a given range. Long maintaining of a constant temperature (not less than 12 h) provided a constant temperature of the layer and absence of convective flows in liquid before the experiment.

The constant temperature of the bottom was kept by a flow of cooling water from a water thermostat into special dish *4*.

To remove not-absorbed admixtures possibly accumulated due to desorption from metal, rubber and other surfaces of absorber and generator, vacuuming was performed through a capillary tube with diameter 1 mm during the whole experiment.

After the valve at the pipeline connecting absorber and generator was open, steam was supplied to the absorber and pressures were usually stabilized in 0.8 s.

During the experiment, temperature was measured at different distances from the bottom, including the interface, the pressure and temperature difference were also measured in the absorber bottom. This information was acquired by PC *5* (Fig. 1). The layer level was measured using cathetometer *6* with an error of 0.01 mm.

At the end of experiment, the valve of steam supply into the absorber was stopped, gas pumping was halted, and atmospheric air was fed in. Then, layer-by-layer drain of solution was performed, and the average density and temperature of each sample and solution as a whole were determined. Concentration was restored by its table dependencies on density and temperature [28] using spline interpolation.

To get data on change of concentration profile in time, a cycle of 12 experiments was carried out. These experiments repeated all initial and current conditions, and they differed by duration (from 15 min to 20.5 h).

6. Experimental results

Experimental parameters and thermal physical properties of solution are presented in Table 1.

Measurement results on temperature profiles in various moments of time are shown in Fig. 2a and b. Temperature dependencies on time at different levels of the absorbent layer and on its surface are presented in Fig. 3a and b in comparison with calculations. In calculation, a quadratic dependency was used as a function describing the equilibrium state at the interface. At the pressure shown in Table 1, this dependency takes the form of $T_i = 180.5 - 414.66C_i + 267.6C_i^2$.

Calculation of temperature inside the layer of solution was carried out with successive consideration of an increase in the film thickness.

These results prove the main theoretical assumptions. Particularly, it is shown that at a constant pressure at some initial moment of time, the temperature of the layer surface slightly differs from a constant predicted theoretically. Then, the temperature at the interface decreases, and the temperature profile inside the layer really approaches the linear one.

Separately, the initial period of the pressure increase and stabilization in the absorber was considered in detail during this experiment. The pressure was measured with a frequency of 1 kHz, temperature was measured with a

Table 1
Thermodynamic properties and parameters

a	1.3×10^{-7}	[$m^2\,s^{-1}$]
ρ	1680	[$kg\,m^{-3}$]
D	1.27×10^{-9}	[$m^2\,s^{-1}$]
r_a	2.725×106	[$J\,kg^{-1}$]
C_p	1980	[$J\,kg^{-1}\,K^{-1}$]
P	1970	[Pa]
μ	6.94×10^{-3}	[$kg\,m^{-1}\,s^{-1}$]
T_0	20.4	[°C]
v	4.117×10^{-6}	[$m^2\,s^{-1}$]
C_0	0.42	
λ	0.415	[$W\,m^{-1}\,K^{-1}$]
T_w	20.4	[°C]

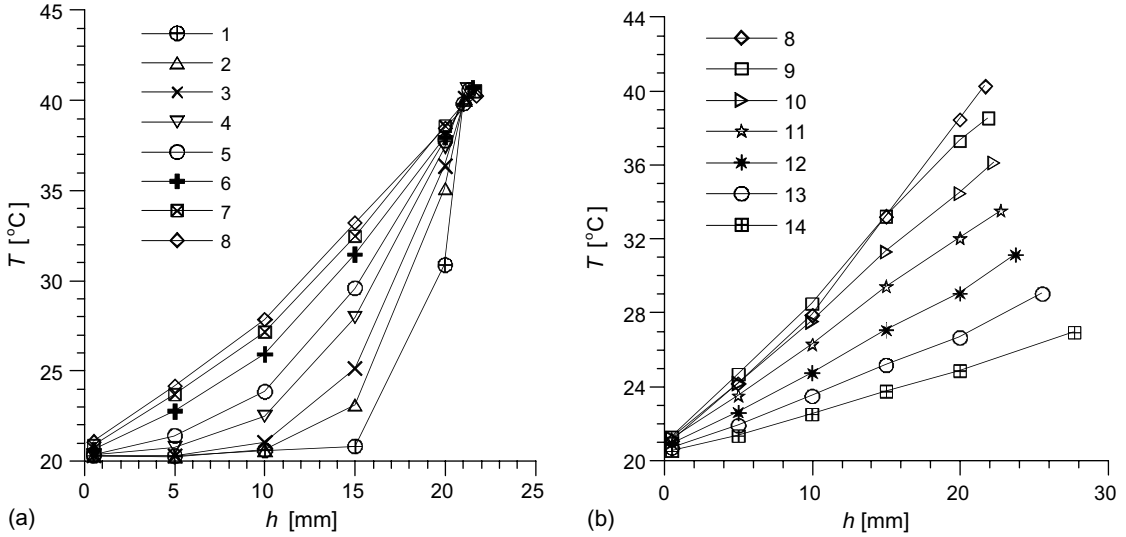

Fig. 2. Temperature profiles for different time moments. (a) 1—$t = 12.6$ s, 2—57 s, 3—101 s, 4—201 s, 5—299 s, 6—501 s, 7—753 s, 8—995 s; and (b) 8—$t = 995$ s, 9—1900 s, 10—4544 s, 11—8748 s, 12—19553 s, 13—41266 s, 14—73692 s.

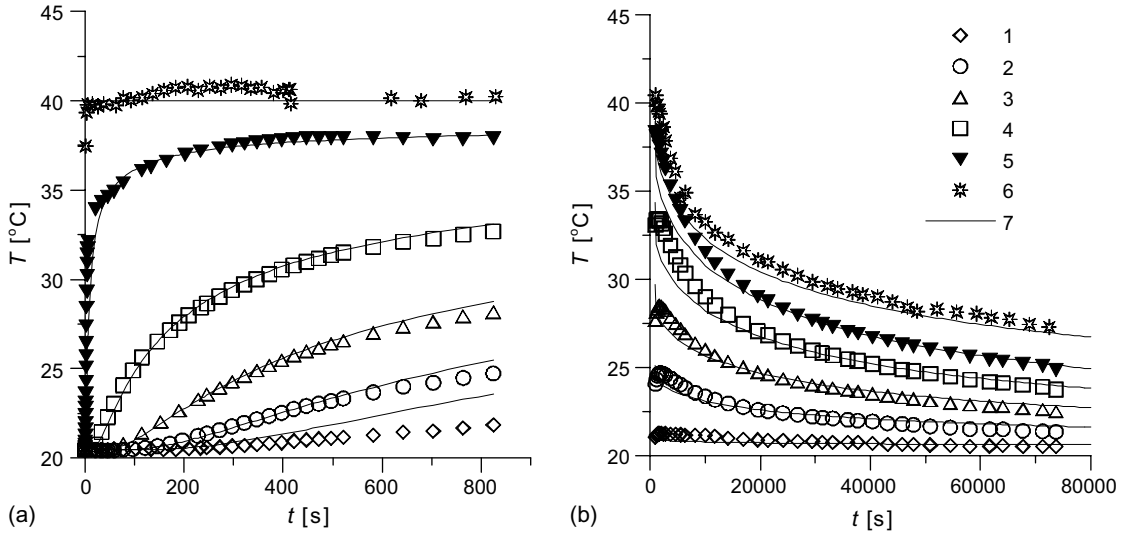

Fig. 3. Temperature evolution at different distances above the bottom (a—small times, b—large times). 1—$h = 0.5$ mm, 2—5 mm, 3—10 mm, 4—15 mm, 5—20 mm, 6—surface, 7—calculations.

frequency of 164 Hz, i.e., IR camera was used in the mode of temperature measurement along a given line only. A frame of IR camera measurement of the initial period is shown in Fig. 4. At calculation of the surface temperature under the mode of changing pressure, we used the solution obtained for short periods, and the quadratic dependency $C_i = f(T_i)$ at the interface corresponded to every value of pressure. Results of these measurements and comparisons with calculation shown in Fig. 5. According to these results, the surface temperature increases with pressure, but calculation values of T_i are slightly higher than the measured ones. This difference is kept for the short period of time, and when the pressure in absorber reaches a constant value, the temperature of a free surface of the layer T_i also becomes constant and almost coincides with the calculated one.

Profiles of concentration at various moments of absorption are shown in Fig. 6, and the measured average value of concentration for each layer corresponds to its average coordinate. Concentration on the

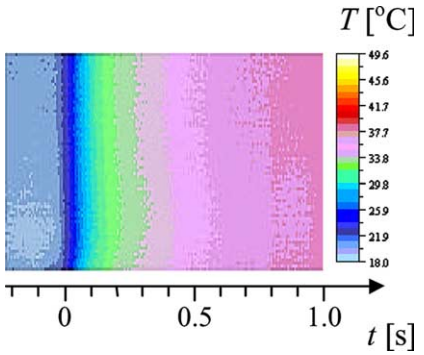

Fig. 4. The staff of IR camera measurements of temperature in an initial stage of time.

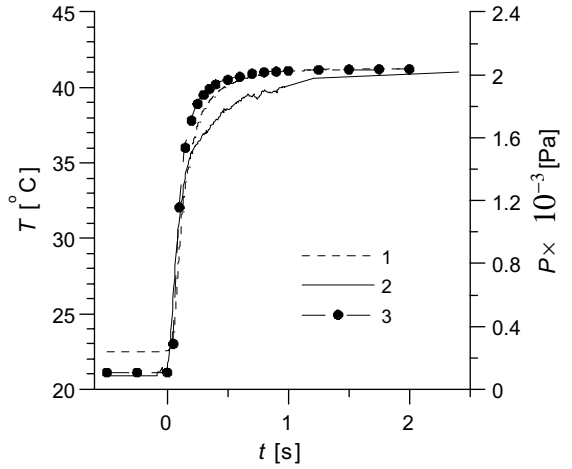

Fig. 5. Change of temperature of a surface and pressure at the initial moment of time. 1—pressure, 2—temperature, 3—temperature calculation.

layer surface was determined by the surface temperature measured by IR camera in accordance with the equilibrium state. At a constant growth in the share of absorbable substance in each layer, the concentration profile changes with time from more concave to less concave.

A change in the layer thickness and absorbable mass with time is shown in Figs. 7 and 8. The calculated values of mass growth are 15–20% less than the measured ones, and this can be explained both by imperfection of the model (especially at high t), insufficient measurement accuracy, and by possible discrepancy between experimental conditions and model assumptions.

Experimental results on time change of bottom temperature, i.e., deviation from the condition of isothermal state of the bottom are shown in Fig. 9. This deviation reaches its maximum (0.26 °C) at the moment

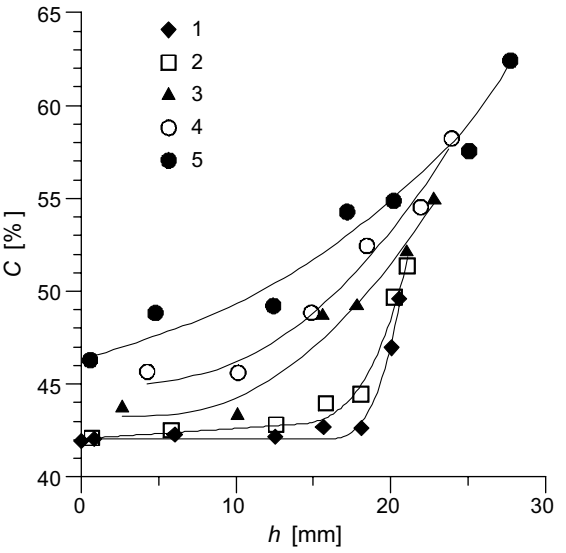

Fig. 6. Concentration profiles for different time moments. 1—$t = 980$ s, 2—3667 s, 3—14,555 s, 4—35,643 s, 5—73,692 s.

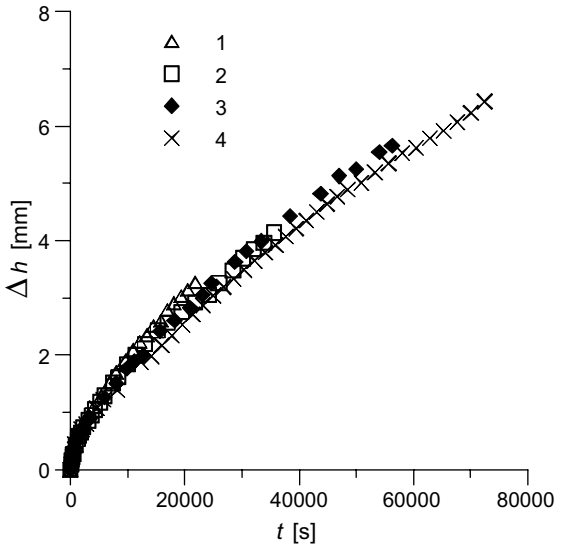

Fig. 7. Change in time of thickness of a layer. 1, 2, 3, 4—experimental data.

of 1500–2000 s. Perhaps, the interval of significant deviation of the bottom temperature from a constant by 400–10000 s, can be firstly correlated with coming of the heat boundary layer to the bottom, and then, with transformation of the temperature profile into the linear form. In this interval, a growth of the heat flux through the bottom surface to its maximal value and back should be observed (for the given experiment, this should be

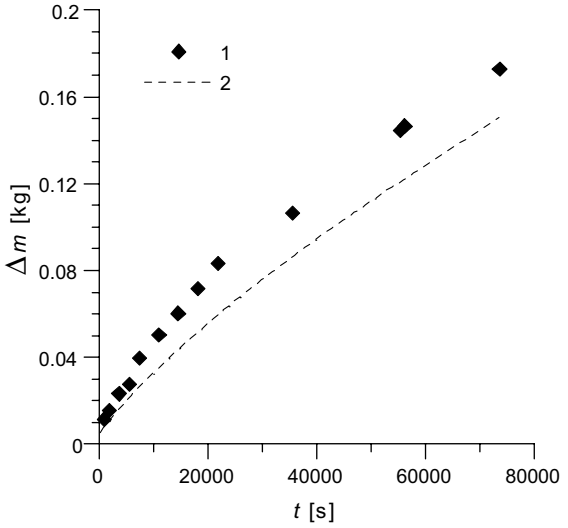

Fig. 8. Mass of absorbed substance vs. time. 1—experimental data, 2—calculations

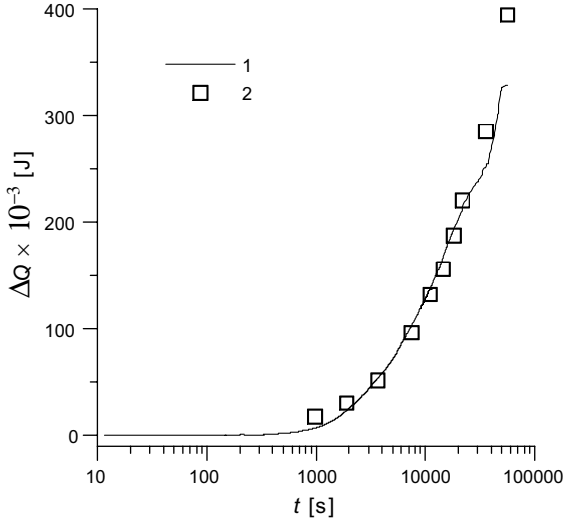

Fig. 10. Thermal balance of an absorber: 1—removed heat, 2—it is warm; allocated as a result of absorption except for the solution spent for heating.

observed from zero since $T_0 = T_w$). In calculations for $t \leqslant 800$ s, we used solution at short periods and for $t > 800$, solution with a linear temperature profile was used. There was no a transition area at calculations. Probably, this led to some difference in calculation and experimental temperature values near the bottom (Fig. 3a).

During the experiment, we checked the balance, which considered heat, generated at absorption, and heat removed through the absorber bottom and spent for solution heating. According to Fig. 10, during 7 h the balance is kept accurately, but then a decrease in the bottom temperature difference to the values comparable with a measurement error and neglecting of heat removal through a lateral wall lead to some imbalance.

Results presented demonstrate perfect correspondence between experimental data and calculations performed using models of mutually connected heat and mass transfer at absorption by an immovable layer of solution. This allows using simple models as the limit or standard ones for analysis of numerical and experimental results obtained under complex physical conditions.

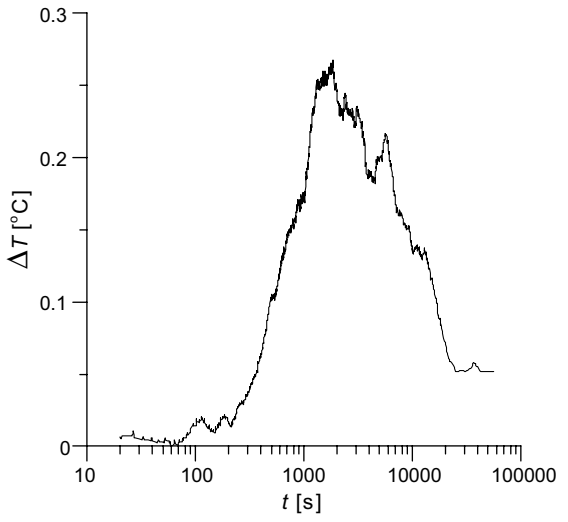

Fig. 9. Temperature drop on the bottom of an absorber.

Acknowledgements

This work was supported financially by the Russian Foundation for Basic Research (grant RFBR 03-02-16393), and executed within the framework of the grant of the President of the Russian Federation on the state support of conducting scientific schools (grant No. NSh-523.2003.1) and the integration project of the Siberian Branch of the Russian Academy of Science No. 133.

References

[1] V.E. Nakoryakov, N.I. Grigorieva, Exact solution to the problem of combined heat and mass transfer at film absorption, J. Eng. Phys. 33 (5) (1977) 893–896.

[2] V.E. Nakoryakov, N.I. Grigorieva, Calculation of heat and mass transfer at non-isothermal absorption at the initial region of a falling film, Theor. Found. Chem. Eng. 14 (4) (1980) 483–488.

[3] G. Grossman, Simultaneous heat and mass transfer in film absorption under laminar flow, Int. J. Heat Mass Transfer 26 (3) (1983) 357–371.
[4] G. Grossman, Heat and mass transfer in film absorption, in: N.P. Cheremisinoff (Ed.), Handbook of Heat and Mass Transfer, Gulf Publishing Co., Houston, TX, 1986, pp. 211–257.
[5] V.E. Nakoryakov, N.I. Grigorieva, Heat and mass transfer at film absorption with a change in volume of a liquid phase, Theor. Found. Chem. Eng. 29 (3) (1995) 242–248.
[6] J.W. Andberg, G.C. Vliet, Design guidelines for water–lithium bromide absorbers, ASHRAE Trans. 98 (1) (1983) 220–232.
[7] G.C. Vliet, J.W. Andberg, A simplified model for absorption of vapors into liquid films flowing over cooled horizontal tubes, ASHRAE Trans. 93 (2) (1987).
[8] J.W. Andberg, G.C. Vliet, Absorption of vapors into liquid films flowing over cooled horizontal tubes, in: Proceedings of the ASME JSME, Thermal Engineering Joint Conference, Honolula, Hawaii, vol. 2, March 22–27, 1987, pp. 533–541.
[9] H. Le Goff, A. Ramadane, P. Le Goff, Modelisation des transferts couples de matiere et de chaleur dans l'absorption gaz–liquide en film ruisselant laminaire, Int. J. Heat Mass Transfer 28 (11) (1985) 2005–2017.
[10] B.J.C. Van der Wekken, R.H. Wassenaar, Simultaneous heat and mass transfer accompanying absorption in laminar flow over a cooled wall, Int. J. Refrig. 11 (1988) 70–77.
[11] B.J.C. Van der Wekken, R.H. Wassenaar, A. Segal, Finite element method solution of simultaneous two-dimensional heat and mass transfer in laminar film flow, Wärme Stoffübertrag. 22 (1988) 347–354.
[12] A.T. Conlisk, Falling film absorption on cylindrical tube, AIChE J. 38 (11) (1992) 1716–1728.
[13] A.T. Conlisk, Analytical solutions for the heat and mass transfer in a falling film absorber, Chem. Eng. Sci. 50 (4) (1995) 651–660.
[14] N. Brauner, D.M. Maron, H. Meyerson, The effect of absorbate concentration level in hygroscopic condensation, Int. Comm. Heat Mass Transfer 15 (1988) 269–279.
[15] N. Brauner, D.M. Maron, H. Meyerson, Coupled heat condensation and mass absorption with comparable concentrations of absorbate and absorbent, Int. J. Heat Mass Transfer 32 (10) (1989) 1897–1906.
[16] N. Brauner, Non-isothermal vapour absorption into falling film, Int. J. Heat Mass Transfer 34 (3) (1991) 767–784.
[17] R. Yang, B.D. Wood, A numerical modeling of an absorption process on a liquid falling film, Solar Energy 48 (3) (1992) 195–198.
[18] V.E. Nakoryakov, A.P. Burdukov, N.S. Bufetov, N.I. Grigorieva, A.R. Dorokhov, Experimental study of non-isothermal absorption by a falling liquid film, Theor. Fund. Chem. Eng. 14 (5) (1980) 755–758.
[19] A.T. Conlisk, Structure of falling film heat and mass transfer on a fluted tube, AIChE J. 40 (5) (1994) 756–766.
[20] S.K. Lee, T. Nagasaki, Water vapor absorption enhancement in LiBr/H_20 film falling on horizontal tubes, Exp. Heat Transfer 4 (1991) 331–342.
[21] G.C. Vliet, F.B. Cosenza, Absorption in falling water/LiBr films on horizontal tubes, ASHRAE Trans. 96 (1) (1990) 693–701.
[22] G.C. Vliet, F.B. Cosenza, Absorption phenomena in water–lithium bromide films, in: Japanese Absorption Heat Pump Conference, Tokyo, Japan, Conference Proceedings, September 30–October 2, 1991.
[23] W. Chen, G.C. Vliet, Effect of inert gas on heat and mass transfer in a vertical channel with falling films, Trans. ASME 119 (1997) 24–30.
[24] Y.-M. Chen, C.-Y. Sun, Experimental study on the heat and mass transfer of a combined absorber–evaporator exchanger, Int. J. Heat Mass Transfer 40 (4) (1997) 961–971.
[25] H. Daiguji, E. Hihara, T. Saito, Mechanism of absorption enhancement by surfactant, Int. J. Heat Mass Transfer 40 (8) (1997) 1743–1752.
[26] S.H. Chang, H.L. Toor, Gas absorption accompanied by a large heat effect and volume change of the liquid phase, AIChE J. 10 (3) (1964) 398–402.
[27] V.E. Nakoryakov, N.I. Grigorieva, Vapor absorption stagnant layer of solution, J. Eng. Thermophys. 11 (1) (2002) 115–127.
[28] H. Löver, Thermodynamischen und physikalische Eigenschaften der wässrigen Lithiumbromid Lösung, Dissertation, Karlsruhe, 1960.